Available online at www.sciencedirect.com

ScienceDirect

Energy Procedia 45 (2014) 1382 – 1391

Energy Procedia

68th Conference of the Italian Thermal Machines Engineering Association, ATI2013

Numerical analysis of a low NOx partially premixed burner for industrial gas turbine applications

Antonio Andreini[a], Bruno Facchini[a], Alessandro Innocenti[a,*], Matteo Cerutti[b]

[a]*Department of Industrial Engineering of Florence (DIEF), University of Florence, Florence 50139, Italy*
[b]*GE Oil&Gas, Via F. Matteucci 2, Florence, Italy*

Abstract

A numerical analysis of a low NOx partially premixed burner for industrial gas turbine applications is presented. In the first part the mixing inside a double annular counter-rotating swirl nozzle where the fuel is injected in a transverse jet configuration is studied. Standard $k-\epsilon$ model and Two variable Schmidt number models were assessed in order to find a reliable configuration able to fit the available experimental profiles. Resulting profiles are used to perform reactive simulations of the experimental test rig, where NOx, CO measurement were available Results are compared in terms of NOx concentration at the outlet with experimental data.

Keywords: Turbulent mixing; Variable Schmidt number; NOx emission;

1. Introduction

The concurrent demand for highly fuel flexible and low NOx emissions gas turbines in Oil&Gas applications has led designers to optimise combustor concept design, with particular attention to the injection system. Several numerical approaches have been developed as well as experimental campaigns have been conducted to assist them. The standard way to get low NOx in modern combustors is the adoption of lean premixed flames (Lean Premixed Combustor, LPC) stabilised by a large recirculation zone rather than a pilot flame. Lean premixed flames allow a more precise control on flame temperature, as well as to avoid non-uniform near-stoichiometric local mixture composition inside the combustor, both these representing fundamental aspects for NOx emissions control. It is clear the importance of the premixing system which also functions as injector. With the aim of obtaining a uniform mixing between fuel and air, cross-flow jet configuration is widely used to enhance mixing in premixers injection systems (see Fig.1). The complex flow field establishing when a transverse jet is present together with the high turbulence levels related non-stationary phenomena generated by the two fluxes interaction, make RANS calculation of cross-flow jets challenging.

* Alessandro Innocenti. Tel.: +39-055-4796618 ; fax: +39-055-4796342.
E-mail address: alessandro.innocenti@htc.de.unifi.it

doi:10.1016/j.egypro.2014.01.145

Nomenclature

Sc Schmidt number
$\widetilde{\phi}_i, \widetilde{\phi''_i}$ Reynolds-averaged scalar and of the turbulent scalar fluctuation
$\bar{\rho}$ Reynolds-averaged density
$\widetilde{u_i}, \widetilde{u''_i}$ i component of the Reynolds-averaged velocity and of the turbulent velocity fluctuation
$\widetilde{x_i}$ i axis of the Cartesiam coordinate system
μ, μ_T molecular and eddy viscosity
$\widetilde{\dot{\omega}_\phi}$ mean scalar source term

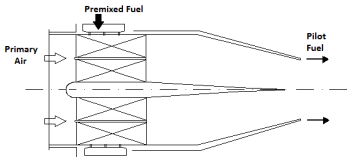

Fig. 1: GE5B1 premixer scheme

The most widespread approach to calculate turbulent scalar transfer is based on Reynolds analogy concept [1]. In this approach, the turbulent Prandtl (Pr_t) and Schmidt (Sc_t) numbers are used to model turbulence effects on scalar transport establishing a proportionality between the momentum transfer and the turbulent scalar transfer. The turbulent scalar flux $\bar{\rho}\widetilde{u''_i\phi''}$ in RANS equations is generally modelled with the gradient diffusion hypothesis

$$\widetilde{u''_i\phi''} = -D_t \frac{\partial\widetilde{\phi}}{\partial x_i} \qquad D_t = \frac{\mu_T}{Sc_t}. \tag{1}$$

where the D_t is turbulent diffusion coefficient. The general scalar ϕ transport equation becomes then:

$$\frac{\partial}{\partial x_i}(\bar{\rho}\widetilde{u_i}\widetilde{\phi}) = \frac{\partial}{\partial x_i}\left[\left(\frac{\mu}{Sc} + \frac{\mu_T}{Sc_t}\right)\frac{\partial\widetilde{\phi}}{\partial x_i}\right] + \widetilde{\omega_\phi} \tag{2}$$

The main advantage using this approach is that it is possible to avoid a full second moment closure for scalar transport being turbulent scalar fluxes computed from the modelled momentum transfer [1]. RANS models tend to underestimate turbulence levels when applied to a cross-flow jet. This limitation is mainly due to their inability to correctly model all the turbulence scales range present in such a configuration as well as the intrinsic hypothesis of isotropy which lies behind most of them. To compensate the effects on turbulent scalar transport it makes necessary the choice of low Pr_t and Sc_t thus increasing D_t. Such considerations may be confirmed by many studies present in literature as in the work of Ivanova et al. [2] where a single 90° jet is simulated with several turbulence models. The author founds that, in case of a $k-\omega$ SST model the Sc_t value which allowed the best agreement with experimental results is 0.25 but this value increase to 0.5 in case of $k-\omega$ SST with curvature correction, this increasing the turbulent kinetic energy. He et al. [3] applied the standard $k-\epsilon$ model for turbulence modelling of jet in cross-flow. In this case the best accuracy was found with a Sc_t of 0.2. In any case such low values are not entirely physical and just help artificially increase turbulent scalar transport [2]. Moreover they are typically assumed constant all over the domain despite many experimental and numerical analysis showed that they are field variables [4].

A Preliminary numerical investigation has been carried out, performing RANS simulations, to assess the turbulence model to correctly predict the mixing inside a double annular counter-rotating swirl nozzle where the fuel is injected in a transverse jet configuration from the outer annulus. To face previously mentioned RANS models limitations, the standard $k-\epsilon$ model has been modified and calibrated in order to find a configuration able to fit the available experimental profiles, obtained at low pressure conditions, at two different locations. A turbulent Schmidt number sensitivity analysis has been then carried on. Moreover two variable Schmidt number models, proposed by Goldberg

et al. [4] and Keistler [5], have been implemented and tested with the aim of overcoming the previously mentioned problems related to a constant Sc_t assumption, and obtaining more physical and reliable results to be given as input for the following reactive simulations.

A correct inlet profiles prediction is crucial for a reliable reactive simulation. In case of lean premixed flame stabilised by rich pilot flames, as the one studied in the present work, several complex aspects need to be faced. The wide range of equivalence ratios, from very lean condition to very rich ones, and the simultaneous presence of both the pilot diffusive combustion modality and the premixer premixed one, make it difficult a proper choice of a combustion model able to deal with all the conditions present at the same time. Flame prediction, flammability limits as well as reactions description become challenging to be attained together in all the domain.

NOx prediction is therefore affected by all the discussed modelling difficulties considering that even a small change in equivalence ratio as well as in temperature levels may severely impact NOx reaction rates and, in turn, overall NOx emission.

2. Fuel injection and turbulent mixing investigation

In the first part of the paper is presented the investigation carried on on fuel (CH_4) injection and turbulent mixing inside the GE 5B1 gas turbine combustor premixer. The turbulence and the variable Schmidt models have been assessed and tested on this latter performing simulations at atmospheric conditions. Results are compared with available Fuel Air Ratio (FAR) profiles at two reference section of 1 mm and 32 mm from the premixer outlet. Experimental tests have been performed by GE Oil &Gas in the same conditions.

2.1. Premixer geometry and numerical setup

The GE 5B1 partially premixed annular combustor injection system in Fig.2 consists in a double annular counter-rotating swirl nozzle. The outer swirler is divided into 10 vanes whilst the inner one into 5. The fuel is injected in a transverse jet configuration from the outer annulus. In its original configuration the injection system is made up by 30 injection holes displaced around the outer swirler. In particular three holes are present on each of the outer swirler vanes. Following the swirler there is a converging nozzle where the mixing is completed, before entering the combustion chamber. Such a design promotes high turbulence levels allowing an intense mixing and an uniform profile at the exit. The premixer periodicity allows the simulation of only 1/5 (72°) of the whole test rig (see Fig.2), making it possible to reduce numerical costs of the simulation. The subdivision was complicated by the presence of two counter-rotating swirler so that was not possible to create a single sector. Two separated sectors were than created, each one following the corresponding swirler rotation, merging them in one sector at the converging nozzle inlet.

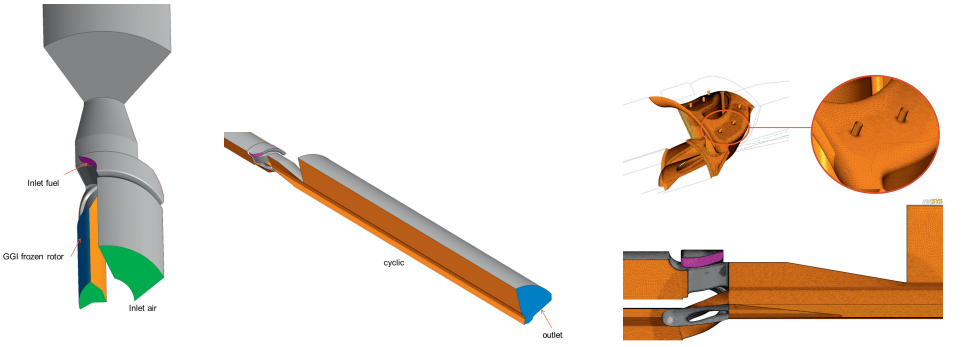

Fig. 2: Premixer geometry and mesh particulars

All the simulations were performed with $ANSYS^{®}CFX$ 14.0 on a 7.2 M elements mesh in Fig.2.

In order to limit calculation instability a CFX specified blend factor scheme [6] with a blend factor of 0.5 has been adopted. The choice of a blend factor of 1 is formally a second-order accurate in space while a blend factor

of 0 is formally equivalent to an upwind scheme. Periodic conditions were assigned on the lateral interfaces while a fluid-fluid interface (Frozen rotor General Grid Interface [6]) is introduced for top and bottom surfaces of respectively inner annulus and outer one. This surfaces in fact represent the same fluid surface portion so flow continuity must be guaranteed. No slip wall condition was assigned on swirler walls, center body and on the converging duct. Air and fuel were introduced in the experimental conditions that is at atmospheric pressure and at a temperature of 293 K. The fuel is directly supplied by the fuel plenum introduced in the simulated domain. An opening boundary condition was instead assigned on the outlet section. Isothermal flow hypothesis is introduced.

2.2. Turbulence modelling

To model turbulence momentum mass transfer in the flow the eddy viscosity, two equation $k-\epsilon$ model has been chosen. For both turbulence kinetic energy k and turbulence eddy dissipation ϵ a transport equation is resolved:

$$\frac{\partial}{\partial x_i}(\bar{\rho}\widetilde{u_i}\widetilde{k}) = \frac{\partial}{\partial x_i}\left[\left(\frac{\mu}{Sc} + \frac{\mu_T}{Sc_k}\right)\frac{\partial \widetilde{k}}{\partial x_i}\right] + \bar{\rho}P - \rho\widetilde{\varepsilon} \tag{3}$$

$$\frac{\partial}{\partial x_i}(\bar{\rho}\widetilde{u_i}\widetilde{\varepsilon}) = \frac{\partial}{\partial x_i}\left[\left(\frac{\mu}{Sc} + \frac{\mu_T}{Sc_\varepsilon}\right)\frac{\partial \widetilde{\varepsilon}}{\partial x_i}\right] + C_{\varepsilon 1}\bar{\rho}\frac{\widetilde{\varepsilon}}{\widetilde{k}}P - C_{\varepsilon 2}\bar{\rho}\frac{\widetilde{\varepsilon}^2}{\widetilde{k}} \tag{4}$$

where Sc_k and Sc_ϵ are the turbulent Schmidt numbers for k and ϵ respectively, P are the production terms, $C_{\epsilon 1}$ and $C_{\epsilon 2}$ modelling constants. For further details refer to [7].

The standard model shows problems related to the underestimation of turbulence levels mainly due to local isotropy hypothesis. High levels of turbulent kinetic energy are present at the shear layer between the two counter-rotating stream The turbulence model is likely to underestimate turbulence levels in this region leading to a less intense turbulent diffusion and mixing. A change in the constant $C_{\epsilon 1}$ in ϵ equation 4 is proposed, leading to a lower turbulence kinetic energy dissipation. After a tuning analysis on such model constant a value of 1.15 (instead of the default one of 1.44) has been proposed. Moreover, a constant lower value of 0.2, instead of the default one of 0.9, is adopted for Sc_k in k equation 3.

2.3. Variable Schmidt models

In order to limit the non-physical hypothesis of isotropy and the assumption of an uniform $Sc_t$of 0.2, two variable Schmidt models has been implemented and tested. The main equations and features of these are described below. For further details refer to [4] for Glodberg's model and to [5] of the second model proposed by Keistler.

2.3.1. Goldberg's model

The proposed algebraic model is a generalization of the approach of Sturgess e McManus [8] which was elaborated based on the isotropy hypothesis. In order to remove isotropy constrain the algebraic Reynolds Stress Model of Rodi, based on the assumption of retaining Reynolds stress transport proportional to those of k [9], is adapted to retrieve a correlation for the term $\widetilde{u_i''\phi''}$ [4]. A second formulation for the same term is also suggested by the author, and used in this work, in case of isotropic turbulence model adoption:

$$\widetilde{u_i''\phi''} = \frac{\tau_t}{C_{\phi 1} + \frac{1}{2}(\frac{P_k}{\varepsilon} - 1)}\left[\widetilde{u_i''u_j''}\frac{\partial \widetilde{\phi}}{\partial x_j} - \frac{C_{\phi 2}}{6R}f_\phi k\tau_t\sqrt{\left(\frac{\partial \widetilde{u_i}}{\partial x_l}\frac{\partial \widetilde{u_i}}{\partial x_l}\right)\left(\frac{\partial \widetilde{\phi}}{\partial x_l}\frac{\partial \widetilde{\phi}}{\partial x_l}\right)}\right] \tag{5}$$

where P_k, τ_t are function of $\widetilde{u_i''u_j''}$, $\widetilde{k}$, $\widetilde{\epsilon}$ and $\frac{\partial \widetilde{u}}{\partial x_i}$, $C_{\phi 1}$ and $C_{\phi 2}$ and R model constants, f_ϕ function of μ, $\widetilde{k}$ and $\widetilde{\epsilon}$. The final expression for the turbulent Schmidt number is

$$\begin{cases} Sc_T = Sc_{T,const}, & \zeta^2 < \lambda \\ Sc_T = max\left\{0.1, min\left[Sc_{T,const}, \psi \max\left\{\sigma_{t1}, \sigma_{t2}\right\}\right]\right\}, & \zeta^2 > \lambda \end{cases} \tag{6}$$

where $\zeta^2 = \frac{\partial\phi}{\partial x_l}$ and $\lambda = 10^{-5}$. The $S\,c_t$ can vary from a lower bound of 0.1 to a maximum one of $S\,c_{T,const}$. ψ constant, whose default value is set to 2.0, has a direct influence on the $S\,c_t$ dependency on the diffusion coefficient D_t which is expressed in terms of σ_{t1} or σ_{t1} as follows [4]:

$$D_t = \left[\sqrt{\frac{(\frac{\partial\widetilde{\phi}}{\partial x_j})(\frac{\partial\widetilde{\phi}}{\partial x_j})}{\widetilde{u_i''\phi''}\widetilde{u_i''\phi''}}}\right]^{-1} \qquad \sigma_{t1} = \frac{\mu_T}{\bar{\rho}}{D_t}^{-1} \qquad \sigma_{t2} = \frac{\sqrt{\widetilde{u_i''u_j''}\widetilde{u_i''u_j''}}}{|S|}{D_t}^{-1} \tag{7}$$

where S is the strain rate tensor.

2.3.2. Keistler model

The second variable Schmidt number model tested in this work is the one proposed by Keistler [5]. The model was originally based on $k-\zeta$ turbulence model proposed by Xiao [10]. Being $\zeta = \epsilon\rho/\mu_T$, the model has been adapted to the $k-\epsilon$ turbulence model. A variable diffusion coefficient D_t definition is retrieved from the resolution of two transport equation for the scalar variance σ_ϕ and its dissipation rate ε_ϕ. D_t definition proposed by the author is:

$$D_t = \frac{1}{2}\left(C_\phi k\tau_\phi + \frac{\mu_T}{\rho\beta_\phi}\right) \qquad \tau_\phi = \frac{\sigma_\phi}{\epsilon_\phi} \tag{8}$$

where β_ϕ, C_ϕ, are model constant [5], while τ_ϕ express the dependency of the diffusion coefficient on σ_ϕ, ε_ϕ.

2.4. Results

Turbulence model assessment and variable $S\,c_t$ analysis results are compared with experimental ones in term of FAR profiles normalized respect to a reference value FAR_{tot} plotted against the radius R normalized respect to the external radius R_{ext}. $R = 0$ represent the domain axis.

Turbulence model assessment has been performed at first, varying model constants ($k-\epsilon$-mod), in order to find a configuration retained reliable for turbulence prediction inside the premixer. Turbulent $S\,c_t$ sensitivity analysis has also been performed. Standard $k-\epsilon$ model with a $S\,c_t$ of 0.2 (Standard $k-\epsilon$-0.2) and the modified model with $S\,c_t$ of 0.2 ($k-\epsilon$-mod-0.2) results are presented in the following.

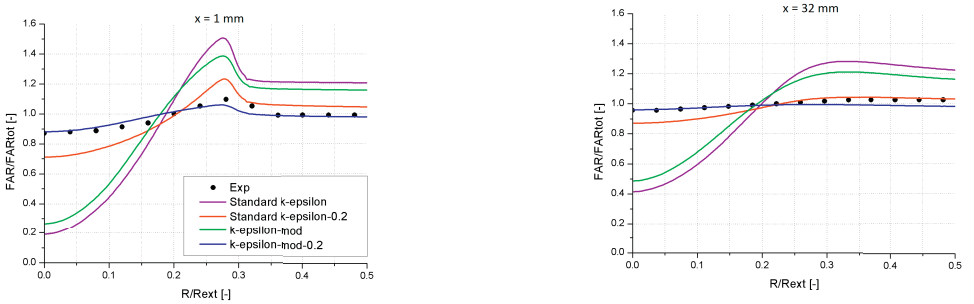

Fig. 3: Normalized FAR profiles obtained with $k-\epsilon$ model at two axial location from premixer exit

Obtained FAR profiles are shown in Fig.3. A slight improvement is introduced tanks to the change in the model constants (green line). A good agreement with experimental results is obtained with the $S\,c_t$change (red line). It is now possible to achieve diffusion toward the premixer axis since the first section at 1 mm from the premixer exit. The peak is caught exactly by all the models but its value now fit the experimental one. Good agreement is obtained also at the 32 mm section. Applying together proposed changes the best agreement with experimental data is achieved at both the locations.

Tab.1 shows the test matrix for simulations with Goldberg's model. The model has been tested at first coupled with the standard $k-\epsilon$ one. A lower bound of 0.1 and upper bound of 0.7 was set for $S\,c_t$. Resulting profiles at both reference section do not show a sufficient diffusion towards lower radius (see Fig. 4).

Table 1: Goldberg's model text matrix

Case name	$k-\epsilon$ version	$Sc_{t,const}$	ψ
Gold-original	standard	0.7	2.0
Gold-mod	modified	0.7	2.0
Gold-mod-1	modified	0.5	1.5
Gold-mod-2	modified	0.5	0.75
Gold-mod-3	modified	0.5	0.55

Table 2: Keistler's model text matrix

Case name	$k-\epsilon$ version	$Sc_{t,max}$	$Sc_{t,mod}$
Keist-original	standard	1.0	1.0
Keist-mod	modified	1.0	1.0
Keist-mod-1	modified	0.7	1.0
Keist-mod-2	modified	1.0	0.7
Keist-mod-3	modified	0.5	1.0

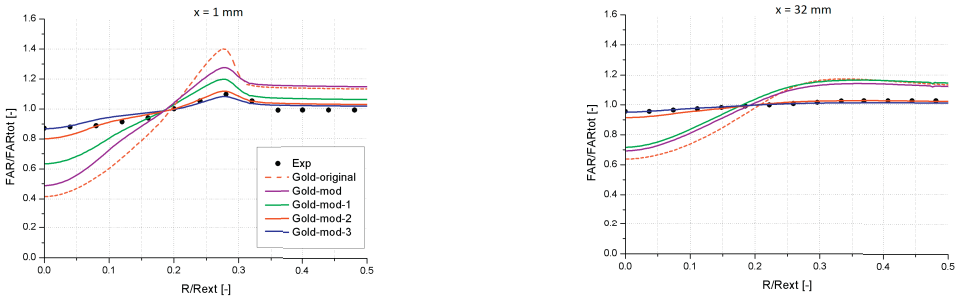

Fig. 4: Normalized FAR profiles obtained with Goldberg's model at two axial location from premixer exit

Using the standard $k-\epsilon$ model underestimation of turbulence levels and low turbulent diffusion and mixing are still present. Goldberg's model has been then coupled with the modified version of the $k-\epsilon$ model (Gold-mod). The effect of the change in the turbulence model constants can be appreciated looking at the profiles in Fig. 4. A sensitivity analysis to the ψ model constant has been carried on in conjunction to a reduction of the maximum Schmidt number $Sc_{t,const}$. ψ change has a direct effect on Schmidt distribution within the chosen limits. The best agreement with experiments is obtained with the Gold-mod-3 configuration. A reduction of Schmidt number is visible in Fig.5 along the shear layer an at the hole exit. The lower values reach the imposed limit of 0.1. It is interesting to notice that there is a large part of the domain not interested by a Sc_t reduction that means a more physical distribution than a global reduction to 0.2 all over the domain. Changing ψ constant improved results can be achieved. The methane now reaches lower radius since the first section (see Fig.4). It is also possible to observe how the peak is caught by all the models. A good agreement is obtained at both the locations.

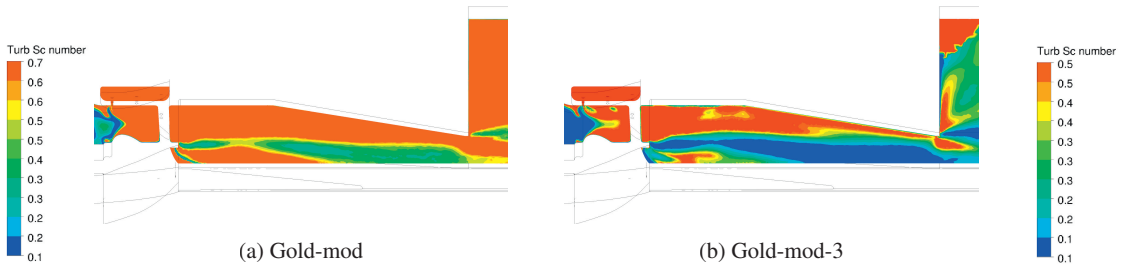

(a) Gold-mod (b) Gold-mod-3

Fig. 5: Turbulent Schmidt number distribution for two of the four configurations of Goldberg's model and modified $k-\epsilon$ model

Keistler's default model has been tested at first coupled with the standard $k-\epsilon$ turbulence model. Again the only Sc_t change is no sufficient to achieve a good match with experiments (see Fig.6). The model has been coupled with the modified $k-\epsilon$. Schmidt number shows still too high values. The effect of the change in the turbulence model constants can be appreciated looking at Fig.6.

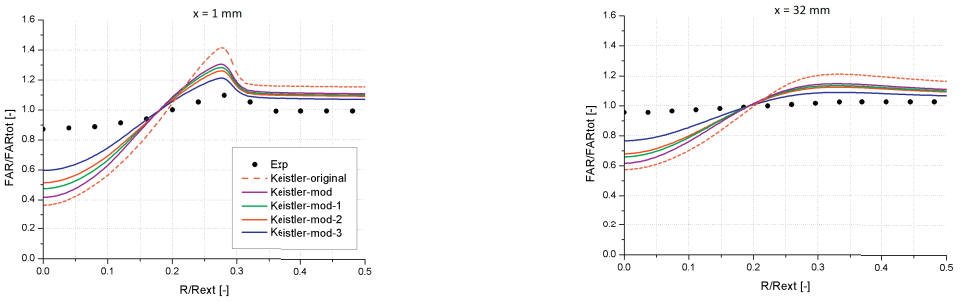

Fig. 6: Normalized FAR profiles obtained with Keistler's model at two axial location from premixer exit

Methane diffusion is still low even though the peak is reduced and more intense diffusion toward the axis is obtained.

To have direct comparison with the previous models, the default maximum Sc_t of 1.0 is lowered (see Tab.2). Two approaches are proposed. The first one is to limit only the second term in D_t definition which is not directly affected by scalar variance. When the scalar variance tends to zero (τ_ϕ tends to 0) Sc_t tends to the imposed limit. The second one is a scaling of the D_t definition acting on both the terms.

$$D_t = \frac{1}{2}\left(C_\phi k\tau_\phi + \frac{\mu_T}{\rho\beta_\phi Sc_{T,max}}\right) \qquad D_t = \frac{1}{2Sc_{T,mod}}\left(C_\phi k\tau_\phi + \frac{\mu_T}{\rho\beta_\phi}\right) \tag{9}$$

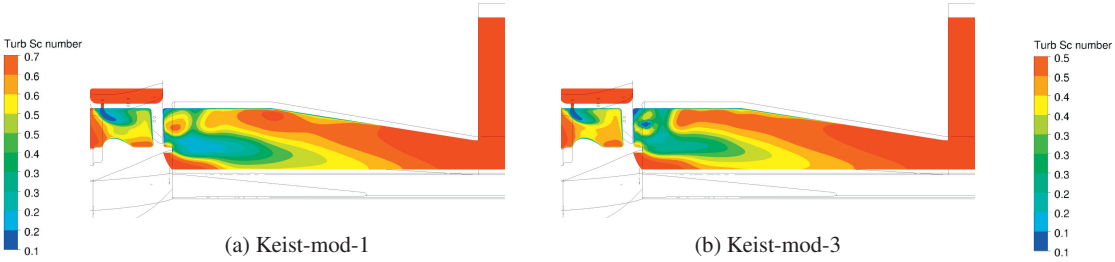

(a) Keist-mod-1 (b) Keist-mod-3

Fig. 7: Turbulent Schmidt number distribution for two of the four configurations of Keistler's model and modified $k-\epsilon$ model

The resulting profiles in Fig.6 are not able to fit experimental results due to the still lower diffusion of methane towards the premixer axis. A slight improved result is obtained with the Keistler-mod-3.

Fig.7 shows Schmidt number distribution for Keistler-mod-1 and Keistler-mod-3. Low Sc_t are present at both the shear layer and at the holes exit. This intense, localized and uniform reduction at the cross-flow jet is an interesting results provided by Keistler's model that was not so marked in Goldberg's model results. The region interested by a Sc_t reduction is wider if compared to the Goldberg model results in Fig.5. On the other hand higher values of Sc_t are obtained with Keistler's model especially along the shear layer. A shorter zone of intense diffusion is predicted by Keistler model.

3. Reactive analysis

Retaining valid the models calibration even when performing simulations at higher pressure, the resulting profiles at different test points have been used to perform reactive simulations at Full Speed Full Load (FSFL) conditions of the experimental test rig, where NOx, CO measurement were available at the combustor outlet.

The $k-\epsilon$-mod-0.2 model has been chosen to retrieve reactive simulation input profiles. These are extracted 9.5 mm backward the premixer exit which identify the premixed mixture inlet in the reactive domain in Fig. 8. Mixture

fraction Z, its variance Z''^2, temperature, turbulence related quantities and velocity components are given as input for reactive simulation after a mean operation along the tangential direction which however does not alter the actual profiles as they are found to be almost uniform along tangential direction.

Table 3: Reactive analysis text matrix

Case name	Fuel split s [%]	ϕ/ϕ_{ref} [-]
Point-0	15	1
Point-1	15	1.08
Point-2	15	0.84
Point-3	25	0.99
Point-4	5	1.01

To do this, several test points have been tested varying both equivalence ratio ϕ and pilot fuel split s. In the test matrix (Tab. 3) the premixer equivalence ratios are scaled by the Point-0 one, taken as reference point. Test points Point-0, Point-1 e Point-2 allow the evaluation of the behaviour varying the premixer equivalence ratio, maintaining constant the pilot fuel split whilst test points Point-0, Point-3 e Point-4 allow the evaluation of the behaviour varying the pilot fuel split, maintaining constant the premixer equivalence ratio.

3.1. Reactive test rig geometry and numerical setup

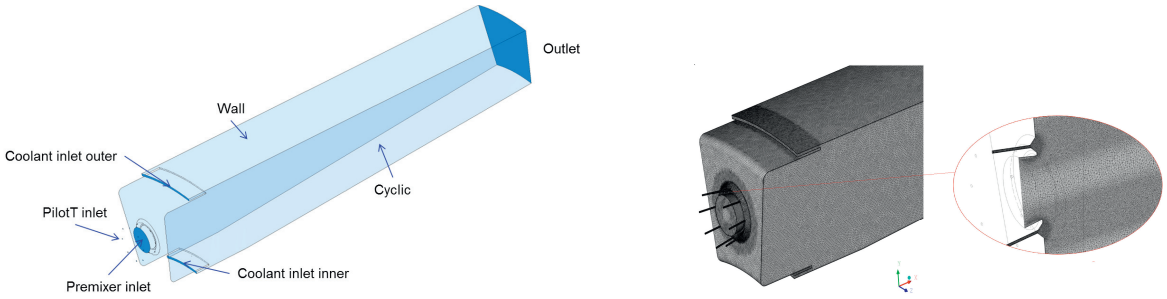

Fig. 8: Reactive test case geometry and mesh

The simulated domain in Fig.8 represents a single sector of annular combustor. The premixer is surrounded by 8 pilot injectors, necessary to stabilise the flame. Inner and outer slot cooling are inserted in the simulated domain. Calculation have been performed with code $ANSYS^{®}CFX$ 14.0 on a 12.3 M cells mesh (Fig. 8) where a localised refinement were realised at the injection system with a progressive coarsening toward the outlet section. After a turbulence model assessment a standard $k-\epsilon$ model has been chosen, where the $C_{\epsilon 1}$ model constant in eq.4 was set to 1.30 to grantee a reasonable turbulence kinetic level inside the domain. Such a change helps limit intrinsic instability and reach convergence, thanks to the higher induced turbulent diffusion. For further details please refer to [11]. A partially premixed combustion model resolving both mixture fraction Z and reaction progress variable c was adopted with Zimont turbulent flame speed closure [6].

As the studied burner is designed to work with very lean mixture at the premixer, close to the lean extinction limit, pilot flame allows flame stabilisation extending equivalence ration range where is possible to have non zero flame speed. An empirical laminar flame speed S_l correlation, based on GE Oil&Gas practices, was adopted in this work being it able to face this aspect with non zero S_l values even at very low equivalence ratios. A constant Sc_t of 0.5 has been used together with a unity Le_t. CH_4 without NOx flamelet was generated from Peters' C2 detailed mechanism available in $CFX^{®}$, with 28 species and 100 reactions [6].

No slip adiabatic wall boundary condition were assigned at the combustor walls. Rotational periodicity was instead assigned on the two lateral surfaces. At pilot and premixer inlet a $c = 0$ boundary condition was assigned while $c = 1$ was set at the coolant inlet to let the combustion be governed by the only flamelet.

NOx emissions was evaluated in terms of NO concentration at the outlet, in a post-processing calculation, considering their influence on the flow-field negligible. The considered NO formation mechanism takes into account Prompt NO (De Soete model for CH_4 [6]) and the extended Zeldovich mechanism with equilibrium hypothesis for O partial equilibrium for OH concentrations. The rate constants are taken from [6]. Turbulence effects are taken into account averaging the laminar reaction rate with local β Probability Density Function (PDF) of temperature. A CFX user subroutine has been implemented to perform the integration. The limits of the pdf integration are determined from the maximum and minimum values of the predicted temperature in the computational domain. The temperature variance (T''^2) equation, necessary to evaluate the PDF, was implemented in the subroutine thus allowing the direct control of each term.

$$\frac{\partial \bar{\rho}\widetilde{T''^2}}{\partial t} + \frac{\partial}{\partial x_i}\left(\bar{\rho}u_i\widetilde{T''^2}\right) = \frac{\partial}{\partial x_i}\left[\left(\frac{\mu_T}{S\,c_{T''^2}}\right)\frac{\partial \widetilde{T''^2}}{\partial x_i}\right] + C_{prod}\frac{\mu_T}{S\,c_t}\left(\frac{\partial \widetilde{T}}{\partial x_i}\right)^2 - C_{diss}\bar{\rho}\frac{\widetilde{\varepsilon}}{\widetilde{k}}\widetilde{T''^2} \tag{10}$$

The default value suggested by [6] are maintained for constants C_{diss}, $S\,c_{T''^2}$ and C_{prod}.

3.2. Results

The predicted flame shape and temperature are shown in Fig.9. Flame shape is close to that observed experimentally: the premixed flame appears to be extended and a thick flame brush is predicted in the final part of the same. The pilot flames introduce instabilities generated by the interaction with the V-shape at the pilot outlet. Temperature distribution clearly shows the peaks due to the rich pilot flames while a core region of fresh unburnt mixture is predicted at the premixer exit. From vector plot in Fig.9b it is clear that the counter-rotating swirlers do not induce a strong enough swirling component to originate a central recirculation zone. The flow is mainly axial except at the two corner regions. The cooling air enters the domain, is convected backward and interacts directly with the pilot flame leading to an oscillation of this latter which is moved towards the premixer flow.

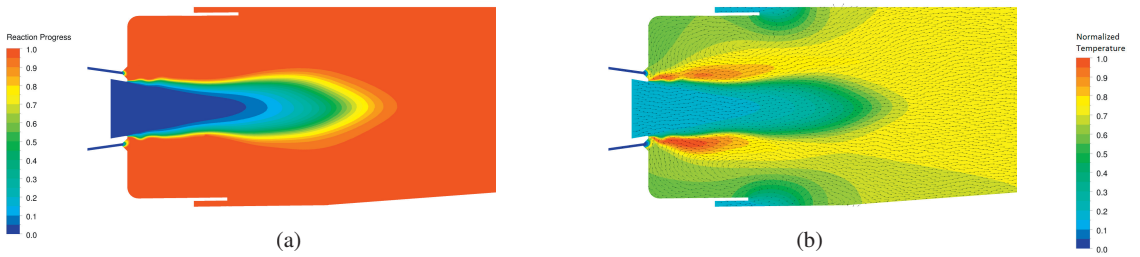

Fig. 9: Point-0 progress variable and mean temperature contours

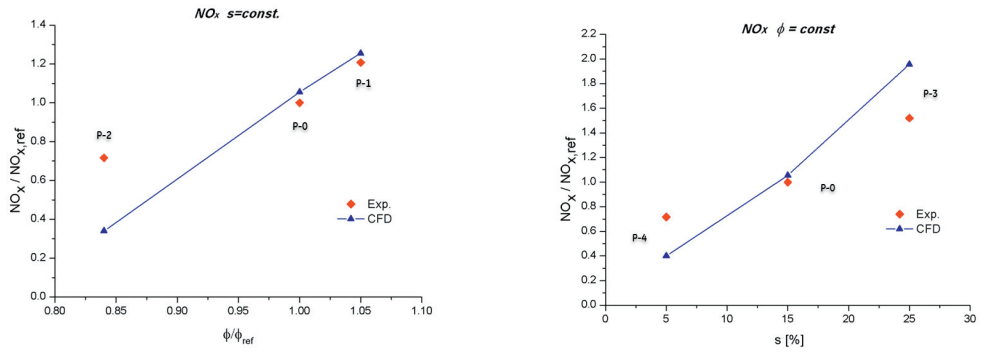

Fig. 10: NOx emissions results

A good agreement was found in emissions trends prediction in Fig.10. The relative variation rate, however, were not accurately predicted by the model. The influence of the premixer on NOx formation rate was found to be marginal

if compared with the pilot flame one. From Fig.10 it is possible to see that lower emissions are predicted for Point-2 at lower load conditions. The mismatching may be due to the not correct prediction of the flame by the combustion model. At very lean conditions it may in fact lead to some difficulties in quenching prediction and in the evaluation of its effects on NOx levels. Under prediction for Point-4 and over prediction for Point-3 are obtained. The result might be due to an erroneous distribution between the relative weight of the different NOx formation mechanisms, in particular a too high sensitivity to thermal formation mechanism. When a very lean flame (Point-2) or a low s case is studied (Point-4), a reduction in temperature levels is predicted and consequently under prediction of NOx levels. Conversely at higher pilot split (Point-3) the numerical model over predicts NOx emissions in conjunction with a increase in temperature levels.

4. Conclusions

A numerical analysis of the low NOx partially premixed burner of GE 5B1 gas turbine for industrial applications has been carried on starting from the turbulent mixing analysis of the premixer, to obtain input profiles for the following reactive simulations, up to pollutant emissions evaluation.

In the first part of the work a turbulence model assessment has been proposed as well as a two variable Sc_t approaches to overcome the underestimation of turbulent mixing, typical of standard models, in case of cross-flow jet configurations. Modified $k-\epsilon$ coupled with both a constant Sc_t of 0.2 and the adapted Goldberg's model give good matching of the experimental data. Keistler's model is not able to fit experiments but predicts a more extended zone of lower Sc_t close to the cross-flow jet. The analysis also resulted in an interesting starting point for further investigation an applications of the adopted models i.e. effusion cooling systems applications.

The second part consists of reactive simulations at FSFL conditions aimed at predicting NO emissions which are eventually compared with available experimental measurements at the outlet. A User subroutine has been set up to perform NO laminar reaction rate averaging to take turbulence-chemistry interaction into account, allowing a direct control on temperature variance equation terms as well as on on integral limits. A good agreement was found in the trends prediction while the relative variation rate were not accurately predicted by the model due to a lack of accuracy in flame prediction at lean condition by the combustion model. The influence of the premixer in the NOx formation rate was found to be marginal if compared with the pilot flame one.

Acknowledgements

This research was supported by the GE Oil&Gas. Many simulations have been performed with the help of Emanuele Burberi during his master thesis.

References

[1] Yang LY, Campbell I Reynolds analogy in combustor modeling. Int J Heat Mass Transf 2008;51/5-6:1251-1263.
[2] Ivanova E, Noll B, Aigner M. 2012. A numerical study on the turbulent schmidt numbers in a jet in cross-flow. Proceedings of ASME Turbo Expo 2012;GT2012-69294.
[3] He G, Guo Y, Hsu AT. The effect of Schmidt number on turbulent scalar mixing in a jet-in-cross-fow. International Journal of Heat and Mass Transfer 1999;42:3727-3738.
[4] Goldberg UC, Palaniswamy S, Batten P,Gupta V. Variable turbulent Schmidt and prandtl number modeling. Engineering Applications of Computational Fluid Mechanics 2010; 4:511-520.
[5] Keistler P. A Variable Turbulent Prandtl and Schmidt Number Model Study for Scramjet Applications. Master's thesis, Graduate Faculty of North Carolina State University; 2009.
[6] ANSYS CFX 14.0. Theory Guide; 2011.
[7] Pope SB. Turbulent Flows. Cambridge University Press. UK; 2000.
[8] Sturgess GJ and McManus KR. Calculation of turbulent mass transport in a bluff-body diffusion flame combustors. AIAA Paper 1984; 84:0372.
[9] Rodi W. Turbulance Models and Their Application in Hydraulics: A State-Of-The-Art Review. University of Karlsruhe, Germany; 1980.
[10] Xiao X, Hassan HA,Baurle RA. Modeling scramjet flows with variable turbulent Prandtl and Schmidt numbers. AIAA Paper 2006;2006:0128
[11] Burberi E. CFD analysis of a low NOx partially premixed burner for industrial gas turbines. Master's thesis, University of Florence, Italy; 2013